European Journal of Medicinal Chemistry 77 (2014) 193–203

Contents lists available at ScienceDirect

European Journal of Medicinal Chemistry

journal homepage: http://www.elsevier.com/locate/ejmech

Original article

Anti-mycobacterial activity of 1,3-diaryltriazenes

Davie Cappoen [a], Jure Vajs [b], Cynthia Uythethofken [a], Andrej Virag [b], Vanessa Mathys [c], Marijan Kočevar [b], Luc Verschaeve [d,e], Martin Gazvoda [b], Slovenko Polanc [b], Kris Huygen [a,*], Janez Košmrlj [b,*]

[a] Scientific Service Immunology, O.D. Communicable & Infectious Diseases, Scientific Institute of Public Health (Site Ukkel), Engelandstraat 642, B-1180 Ukkel, Belgium
[b] Faculty of Chemistry and Chemical Technology, University of Ljubljana, Aškerčeva 5, SI-1000 Ljubljana, Slovenia
[c] Program Tuberculosis and Mycobacteria, O.D. Communicable & Infectious Diseases, Scientific Institute of Public Health (Site Ukkel), Engelandstraat 642, B-1180 Ukkel, Belgium
[d] Program Toxicology, O.D. Public Health and Surveillance, Scientific Institute of Public Health (Site Elsene), J. Wytsmanstraat 14, B-1050 Brussels, Belgium
[e] Department of Biomedical Sciences, University of Antwerp, Universiteitsplein 1, B-2610 Wilrijk, Belgium

ARTICLE INFO

Article history:
Received 9 December 2013
Received in revised form
19 February 2014
Accepted 28 February 2014
Available online 1 March 2014

Keywords:
1,3-Diaryltriazene
Tuberculosis
Antibiotic lead
Acute toxicity
SAR
Genotoxicity

ABSTRACT

The rapid generation and spread of the drug resistant tuberculosis has led to an ongoing demand for novel compounds for therapeutic use. Identification and study of compounds with the ability to inhibit *Mycobacterium tuberculosis* is of paramount importance. For this reason, a library of substituted 1,3-diaryltriazenes based on the acting component of the anti-trypanosomal drug, diminazene aceturate was created and evaluated for its potential as anti-tubercular agent. Several compounds were identified with sub-micro molar inhibitory concentrations against *M. tuberculosis* and other clinically relevant mycobacterial species such as *Mycobacterium bovis*, *Mycobacterium avium* and *Mycobacterium ulcerans*. Although the library of the compounds showed a considerable acute cytotoxicity, a genotoxicity could not be observed. Finally, the triazene **14** was selected with the best biological properties ($IC_{50} = 3.26$ μM, $NI_{50} = 24.22$ μM, $SI = 7.44$). The compound **14** showed the ability to inhibit the growth of intracellular replicating and multi-drug resistant *M. tuberculosis*. The results suggest the molecule to be an interesting scaffold for further study and optimization.

© 2014 Elsevier Masson SAS. All rights reserved.

1. Introduction

Identification and development of the compounds to target *Mycobacterium tuberculosis*, the etiological agent of tuberculosis, is still of utmost importance. According to the figures presented by the World Health Organization (WHO) in 2013 this report states that about 8.6 million people fell ill with TB in 2012 from which 450,000 with multidrug-resistant pulmonary TB. Although more rapid diagnosis and treatment have decreased the mortality by 45% since 1990, 1.3 million patients died, including 320,000 people that were TB/HIV confected. TB is still one of the greatest killers worldwide due to a single infectious agent, second only to HIV/AIDS [1]. Apart from the reports on antibacterial and antifungal activity [2], triazenes are best represented in cancer chemotherapy [3]. Dacarbazine (5-(3,3-dimethyl-1-triazenyl)imidazole-4-carboxamide) (Chart 1, structure a), a synthetic analogue of the naturally occurring purine precursor 5-amino-1H-imidazole-4-carboxamide, and temozolomide (4-methyl-5-oxo-2,3,4,6,8-pentazabicyclo-[4.3.0]nona-2,7,9-triene-9-carboxamide) (Chart 1, structure b) are both antineoplastic compounds [4–6]. As alkylating agents, both compounds share a similar mechanism of action by methylating DNA at the N-7 or O-6 positions of guanine residues. This methylation causes somatic point mutations represented by C:G → T:A transitions in the DNA helix and finally triggers the death of tumour cells [6,7]. The library of 1,3-diaryltriazenes presented in this study are based on the structure of diminazene (4-[2-(4-carbamimidoylphenyl)iminohydrazinyl]-benzenecarboximidamide; Chart 1, structure c), the acting component of the anti-trypanosomal drug diminazene aceturate. The activity of diminazene against protozoa is based on its capacity of minor groove binding to RNA and DNA duplexes [8]. It has been shown that diminazene can act as an antiviral compound, but shows weak potential as antitumour agents [9]. Potential DNA binding properties rise caution in TB chemotherapy, in which patients are treated

* Corresponding authors.
E-mail addresses: kris.huygen@wiv-isp.be (K. Huygen), janez.kosmrlj@fkkt.uni-lj.si (J. Košmrlj).

http://dx.doi.org/10.1016/j.ejmech.2014.02.065
0223-5234/© 2014 Elsevier Masson SAS. All rights reserved.

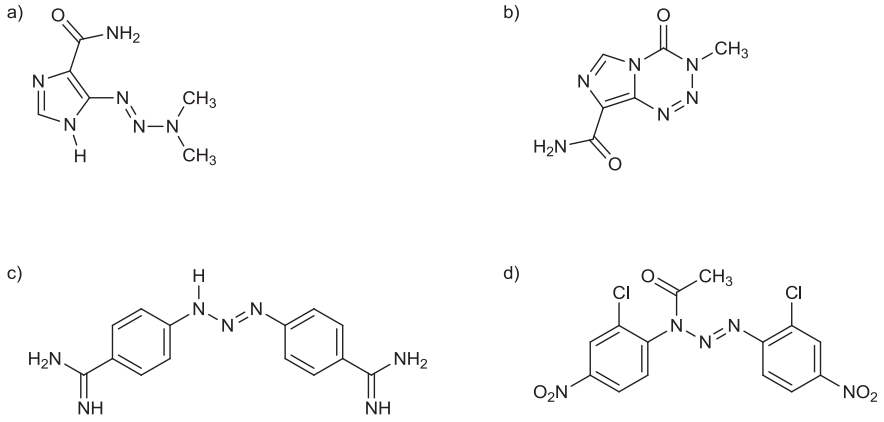

Chart 1. The structures of: a) dacarbazine, b) temozolomide, c) diminazene and d) 3-acetyl-1,3-*bis*(2-chloro-4-nitrophenyl)triazene [10].

for several months. However, observations by Čimbora-Zovko et al. report on a halogen-substituted analogue which did not bind into the minor grove of DNA but instead induces reactive oxidative species [10] (Chart 1, structure d). In this work, we have evaluated a library of twenty-six 1,3-diaryltriazenes, substituted with different electron-withdrawing groups (bromo, chloro, fluoro, nitro, cyano and trifluoromethyl) at the benzene ring.

2. Results and discussion

2.1. Chemistry

The structures of 1,3-diaryltriazenes and their *N*-acyl substituted derivatives tested in this study are shown in Fig. 1.

Several triazenes were synthesized as described before (**2** [10], **10** [10], **11** [10], **14** [11], **15** [12], **16** [13], **17** [14], **18** [11], **19** [10], **20** [15] and **24** [10]). Most of them were recently examined for their antitumour activity [10]. New 1,3-diaryltriazenes were prepared from the corresponding substituted anilines on treatment with either sodium nitrite in hydrochloric acid or with isopentyl nitrite in dichloromethane (Scheme 1). An introduction of the acyl functionality to the triazene nitrogen of the 1,3-diaryltriazene was achieved using the appropriate acid chloride in the presence of triethylamine (Scheme 1).

An attempt to obtain 1,3-diaryltriazene **9a** from 4-fluoro-3-nitroaniline in dichloromethane as a solvent resulted in a complex mixture of products, which was not analysed further. When 4-fluoro-3-nitroaniline reacted with isopentyl nitrite in a mixture of toluene/petroleum ether (1:1), the triazene **9** was formed (Scheme 2). It is the product of S_NAr displacements of one of the fluorine atoms at the initially formed triazene **9a** with the starting aniline. An alternative pathway that first involves the substitution of the fluorine atom at the starting aniline with another molecule of aniline and subsequent reaction with diazonium salt is ruled out. Namely, 4-fluoro-3-nitroaniline remains unchanged in toluene/petroleum ether solution (1:1) at rt for 2 days.

2.2. Biology

In previous publications, we and others have shown that luminometry is a rapid and reproducible tool to test the antimycobacterial activity of novel anti-tuberculous compounds [16–19]. Screening the library of compounds for *in vitro* activity against *M. tuberculosis* was done with the luminescent *M. tuberculosis* H37Rv laboratory strain ($H37Rv^{lux}$). The $H37Rv^{lux}$ strain has multiple copies of pSMT1 plasmid carrying the necessary genes to express the ATP independent bacterial luciferase of *Vibrio harveyi* driven by a constitutive hsp60 promoter. The addition of the luciferase substrate *n*-decanal, elicits a luminescent signal of green-blue light (490 nm) which can be measured by luminometry. The influence of the compounds or other xenobiotics on the bacillary growth can be measured as a reduction in the intensity of the luminescent signal. Serial dilutions of the investigated compounds were used to calculate the concentrations at which 50% (IC_{50}), 90% (IC_{90}) and 99% (IC_{99}) of the *M. tuberculosis* growth was inhibited after 6 days. The IC_{50} of the compounds against *M. tuberculosis* was used to derive a structure activity relation as shown in Table 1. It was observed that the position and nature of the electron-withdrawing substitution group at the 1,3-diaryltriazene largely influenced the activity. Comparing the active compounds **2**, **10** and **13** (IC_{50} = 1.58, 0.03 and 0.57 μM) of the 1,3-diaryltriazenes with the compounds **19** and **20** (IC_{50} = 2.82 and 0.06 μM) of the 3-acetyl-1,3-diaryltriazenes and the compounds **25** and **26** (IC_{50} = 1.69 and 1.45 μM) of the 3-[(2*E*)-3-arylprop-2-enoyl]-1,3-diaryltriazenes we could observe that all compounds with a nitro substitution at the *para* position R^4 showed an increased potency to reduce the *in vitro* *M. tuberculosis* growth at sub-micro molar concentrations. Likewise, comparing the compound **10** (IC_{50} = 0.03 μM) with the analogues **5** and **11** (IC_{50} = 85.51 and 92.96 μM) in which the NO_2 groups were replaced with a halogen F and Cl respectively, the potency was reduced for the latter two molecules.

The compounds **1**, **8**, **12**, **13** and **14** (IC_{50} = 6.88, 6.26, 0.77, 1.97 and 3.26 μM) with a CF_3 group at the *meta* position R^3 also showed increased activity over their analogues. When the CF_3 group was moved from the meta R^3 position to the *ortho* position R^2 (compounds **3** and **5** (IC_{50} = 58.94 and 85.51 μM)) the activity against *M. tuberculosis* was abrogated. An exception to this rule was the compound **10** (IC_{50} = 0.03 μM), which was substituted with a CF_3 group at the *ortho* R^2 position but as mentioned, the compound **10** carried an electron-withdrawing group NO_2 at the *para* R^4 position. Analogues synthesized with both NO_2 and CF_3 substitutions, the compounds **10** and **13**, showed IC_{50} values of respectively 0.03 and 0.57 μM. The compound **10** was even more potent *in vitro* against *M. tuberculosis* in this experiment than the first line *M. tuberculosis* drug INH (IC_{50} = 0.04 μM), used as a positive control in this assay.

An acute toxicity of the compounds was examined in a Neutral Red dye Uptake assay (NRU), shown in Table 1 [20]. This test method makes use of the ability of living cells to bind and incorporate neutral red in their lysosomal structures. The J774 A.1 murine macrophage cell line was selected as a cellular model, macrophages being the primary host cell for *M. tuberculosis*. A toxicity was measured as reduced uptake of the neutral red dye by

1,3-Diaryltriazenes

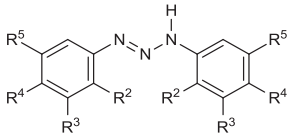

1 $R^2 = F$; $R^3 = CF_3$; $R^4 = R^5 = H$
2 $R^2 = F$; $R^4 = NO_2$; $R^3 = R^5 = H$
3 $R^2 = F$; $R^5 = CF_3$; $R^3 = R^4 = H$
4 $R^2 = CN$; $R^3 = F$; $R^4 = R^5 = H$
5 $R^2 = CF_3$; $R^4 = F$; $R^3 = R^5 = H$
6 $R^2 = CN$; $R^4 = F$; $R^3 = R^5 = H$
7 $R^3 = CN$; $R^4 = F$; $R^2 = R^5 = H$
8 $R^3 = CF_3$; $R^4 = F$; $R^2 = R^5 = H$
9 See, Scheme 2
10 $R^2 = CF_3$; $R^4 = NO_2$; $R^3 = R^5 = H$
11 $R^2 = CF_3$; $R^4 = Cl$; $R^3 = R^5 = H$
12 $R^3 = CF_3$; $R^4 = CN$; $R^2 = R^5 = H$
13 $R^3 = CF_3$; $R^4 = NO_2$; $R^2 = R^5 = H$
14 $R^3 = CF_3$; $R^4 = Cl$; $R^2 = R^5 = H$
15 $R^2 = CN$; $R^5 = CF_3$; $R^3 = R^4 = H$
16 $R^2 = Cl$; $R^5 = CF_3$; $R^3 = R^4 = H$
17 $R^2 = R^4 = Cl$; $R^3 = R^5 = H$
18 $R^3 = R^4 = Cl$; $R^2 = R^5 = H$

3-Acetyl-1,3-diaryltriazenes

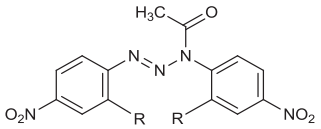

19 R = F
20 R = Br

3-[(2*E*)-3-arylprop-2-enoyl]-1,3-diaryltriazenes

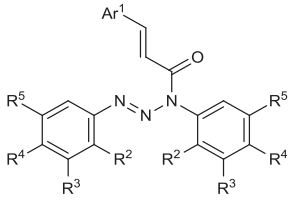

21 $R^2 = CF_3$; $R^4 = Cl$; $R^3 = R^5 = H$; Ar^1 = 2,4-di-OMe-C_6H_3
22 $R^3 = CF_3$; $R^4 = Cl$; $R^2 = R^5 = H$; Ar^1 = 2,4-di-OMe-C_6H_3
23 $R^3 = CF_3$; $R^4 = Cl$; $R^2 = R^5 = H$; Ar^1 = 3,5-di-OMe-C_6H_3
24 $R^2 = Cl$; $R^5 = CF_3$; $R^3 = R^4 = H$; Ar^1 = 2,4-di-OMe-C_6H_3
25 $R^2 = Cl$; $R^4 = NO_2$; $R^3 = R^5 = H$; Ar^1 = 3-OMe,4-OAc-C_6H_3
26 $R^2 = Br$; $R^4 = NO_2$; $R^3 = R^5 = H$; Ar^1 = 3-OMe,4-OAc-C_6H_3

Fig. 1. Structures of 1,3-diaryltriazenes and their *N*-acyl derivatives.

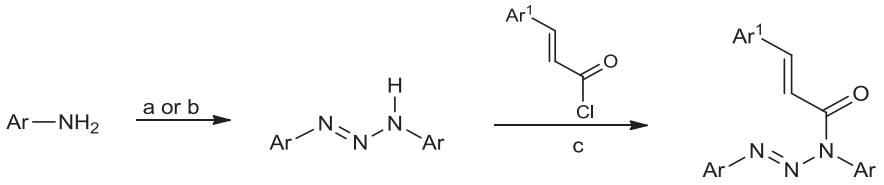

Scheme 1. The synthesis of 1,3-diaryltriaezenes and their *N*-acyl derivatives. Reagents and conditions: (a) $ArNH_2$ (1 mmol), $NaNO_2$ (0.5 mmol)/H_2O (3 mL), 5% HCl (2.5 mL), 0 °C then rt for 18–33 h; (b) $ArNH_2$ (1 mmol)/CH_2Cl_2 (4 mL), *i*-PeONO (1 mmol)/CH_2Cl_2 (4 mL), 0 °C then rt for 0.5–22 h; (c) 1,3-diaryltriazene (1 mmol), acid chloride (1.1 mmol), Et_3N (2 mmol) in acetone (5 mL), rt, 5–40 min.

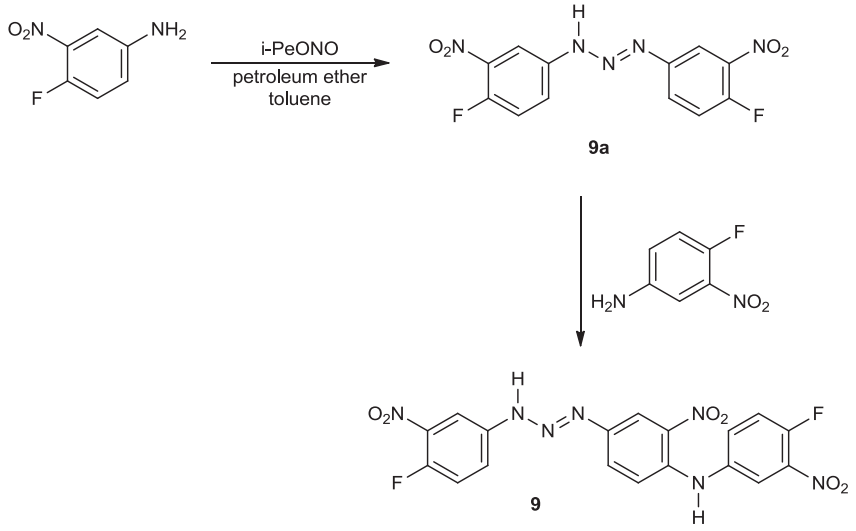

Scheme 2. Formation of the triazene **9**.

Table 1
Growth inhibition of *M. tuberculosis* by the triazene analogues and acute toxicity against macrophages.

Cmpd.	IC_{50}[a]	IC_{90}[b]	IC_{99}[c]	NI_{50}[d]	SI[e]
		(μM)			NI_{50}/IC_{50}
1	6.88	13.41	23.90	52.68	7.7
2	1.58	4.12	9.53	11.63	7.5
3	58.94	>100.00	>100.00	N.D.[f]	N.D.
4	62.34	>100.00	>100.00	N.D.	N.D.
5	85.51	>100.00	>100.00	N.D.	N.D.
6	15.51	20.36	26.02	28.18	1.8
7	>100.00	>100.00	>100.00	N.D.	N.D.
8	6.25	13.41	16.77	26.03	4.2
9	95.66	>100.0	>100.0	21.10	0.2
10	0.03	0.54	1.54	0.61	26.2
11	92.96	>100.00	>100.00	N.D.	N.D.
12	1.97	4.22	10.02	2.09	6.22
13	0.57	6.80	10.25	6.87	10.72
14	3.26	6.47	7.68	24.22	7.44
15	4.57	7.77	15.49	9.69	2.12
16	97.48	>100.00	>100.00	N.D.	N.D.
17	>100.00	>100.00	>100.00	N.D.	N.D.
18	6.81	26.86	72.06	55.22	8.12
19	2.82	8.27	21.96	12.90	4.55
20	0.06	0.64	1.58	1.07	17.47
21	83.13	>100.0	>100.0	N.D.	N.D.
22	52.02	80.77	84.41	N.D.	N.D.
23	71.28	>100.0	>100.0	N.D.	N.D.
24	72.33	>100.0	>100.0	N.D.	N.D.
25	1.69	4.37	9.21	5.12	3.04
26	1.45	3.83	8.41	3.94	2.7
INH[g]	0.04	0.11	0.13	N.D.	N.D.

[a,b,c]The concentration of the analogues at which respectively a growth inhibition of 50%, 90% and 99% of the *M. tuberculosis* H37Rv lab strain was observed as compared to the negative control. Presented results are the mean of triplicate values with a SD < 10%.

[d] The concentration of the analogues at which viability of the macrophages was reduced by 50%. Presented results are the mean of eight replications with a SD < 10%.

[e] The selectivity index (*SI*), calculated by dividing the NI_{50}^{d} by the IC_{50}^{c}.

[f] N.D. Not Done.

[g] INH, one of the first line *M. tuberculosis* antibiotics, isoniazid used as a positive control.

the macrophage culture and the NI_{50} was determined as the concentration at which this reduction reaches 50%. The selectivity index (*SI*) was calculated as a function of the NI_{50} divided with the IC_{50}. An acute toxicity against the J774 macrophages caused by the compounds was studied for compounds with IC_{90} values below 10 μM. For most compounds a 50% reduction in viability of the macrophages was reported at concentrations lower than 30 μM except for the 1,3-diaryltriazenes **1** and **18** (NI_{50} = 52.68 and 55.22 μM), which carry different substitutions. The compounds with the NO_2 group at the R^4 position that were observed to have a strong potency, showed also a high acute toxicity with NI_{50} values below 10 μM. The compound **9** (NI_{50} = 21.10 μM) showed a reduced toxicity by half. For practical reasons, all compounds with a calculated selectivity index lower than the arbitrarily chosen value 7 were excluded from further studies.

Next, the susceptibility of other clinically relevant mycobacterial species was tested as shown in Table 2 for the compounds with an acceptable selectivity index. *Mycobacterium bovis*, together with *Mycobacterium africanum* and *Mycobacterium microti*, constitute the *M. tuberculosis* complex. *Mycobacterium avium* subsp. *avium* is pathogenic for birds but can cause opportunistic infections in AIDS patients, whereas *M. avium* subsp. *paratuberculosis* is the etiological agent of Johne's disease or paratuberculosis (in ruminants) which may be linked to Crohn's disease in humans. *Mycobacterium ulcerans* causes Buruli ulcer, a necrotizing skin disease affecting mostly children in certain rural areas of West-Africa, and may lead to irreversible disabilities when left untreated [21–24]. The study showed that the other mycobacterial species were also susceptible to the 1,3-diaryltriazene compounds at concentrations comparable to that of *M. tuberculosis*. However, the low IC_{50} values observed for *M. tuberculosis* and (to a slightly lesser extent) for *M. bovis* for the compounds **10** and **20** (IC_{50} = 0.03 and 0.06 μM), could not be observed for the other mycobacterial species.

Because the DNA intercalating properties of diminazene, the danger of genotoxicity was addressed. Early signs of genotoxicity can be observed by studying the activation of DNA repair mechanisms. The regulatory SOS operon is a key to the repair of early cellular DNA damage and its activation is mediated by a multiple component system. As a result of DNA interruption, binding of ssDNA fragments to the recA protein increases the enzymatic affinity for the lexA repressor protein. The decrease in lexA frees the SOS box consensus sequence and thereby facilitates the binding of the general transcription machinery to the *recN* promotor sequence and transcription of the SOS operon. Based on this molecular mechanism, the VITOTOX™ model from Gentaur can detect activation of the SOS operon by an integrated lux operon [25]. The model employs two recombinant *Salmonella typhymurium* reporter strains. The integrated lux operon of the Genox strain T104 (recN2-4) is expressed under transcriptional control of the *recN* promoter and in the Cytox *pr1* strain it is driven by the strong constitutive *pr1* promotor, the latter strain mainly functioning as an internal control. Both recombinant reporter strains lack the necessary oxidative machinery to metabolize xenobiotics. By the addition of the S9 liver fraction the genotoxicity of the investigated substance can be distinguished from that of its metabolites. Closely correlated with the AMES test (91%), with a high specificity of 94%, this model allows an early elimination of novel compound classes due to genotoxicity.

Emission of luminescence by the strains was recorded in real time after the addition of the compounds every 5 min during a 4 h period. Compounds were tested at 25.00 μM, 2.50 μM and 0.25 μM in the presence and absence of the metabolizing S9 fraction. Genotoxicity was deduced from the signal to noise ratio (S/N), being the

Table 2
The 50% *in vitro* growth inhibitory concentration of the derivatives against other *Mycobacteria*.

Compound	*M. tuberculosis* H37Rv^{lux}	*M. bovis* AN5^{lux}	*M. avium* ssp. *paratuberculosis* ATCC19698^{lux}	*M. avium* ssp. *avium* ATCC15769^{lux}	*M. ulcerans*1615^{lux}
	50% Growth inhibition (μM)				
1	6.88	8.15	7.80	8.75	21.38
2	1.55	1.30	2.44	2.10	3.37
10	0.03	0.28	0.64	0.38	0.59
13	0.57	0.76	0.99	0.88	1.06
14	3.26	5.50	4.13	7.99	10.74
18	6.81	6.24	10.24	11.90	12.72
20	0.06	0.31	0.45	0.37	1.62

In vitro growth inhibition was measured by luminometry after 6 days exposure to the compounds. Inhibition calculated from triplicates cultures (SD values < 10%).

light produced by the bacterial suspension exposed to the compounds divided by the light produced by a non-exposed bacterial suspension. S/N values for the Genox (recN2-4) higher than 1.5 were interpreted as positive and implied genotoxic properties by the compounds. For the Cytox (pr1) strain, S/N values above 1.5 are considered as direct influence of the compound on the bacterial luciferase or the luminescent signal itself and regarded a false positive. S/N values lower than 0.8 for the Cytox strain are indicative of direct cytotoxicity and exclude false negatives. As shown in Fig. 2, the compounds **1**, **2**, **10**, **13**, **14**, **18** and **20** resulted in values of the Cytox control strain between 0.8 and 1.5 with and without the S9 liver extract. The luminescence emitted from the Genox strain did not exceed S/N values significant higher as 1.5 after addition of the compounds in absence and presence of the S9 extract. However, when the Genox strain was incubated together with S9 and the compounds **2**, **18** or **20** the luminescent signal increased, exceeding 1.5, indicating activation of the SOS operon as a sign of early genotoxicity caused by the metabolites of the compounds **2**, **18** and **20**. No genotoxicity was found for the compounds **1**, **10**, **13** and **14** both in the absence and in the presence of the S9 liver fraction. Regarding the structural differences between the group of **2**, **18** and **20** and the group of **1**, **10**, **13** and **14** it was noticed that all members of the latter group carried CF_3 moiety while none had a CF_3 side chain in the former group.

To investigate the importance of the CF_3 side chain for the protection against degradation, as well as to assess the metabolic stability of the candidate, the potency of the molecules was evaluated when incubated together with S9. The concentration at which a 90% growth reduction of *M. tuberculosis* could be observed by the compounds was measured both in the absence and in the presence of the S9 fraction as shown in Fig. 3. It was confirmed that the potency of the compounds **2**, **18** and **20**, the derivatives without the CF_3 moiety, was reduced significantly by the addition of the S9 liver fraction $p < 0.0001$. This resulted in increased IC_{90} values for these compounds: for compound **2** the IC_{90} rose from 3.84 ± 0.35 μM to 7.95 ± 0.48 μM in the presence of S9. For the derivative **18** the IC_{90} rose from 26.75 ± 0.24 μM to 67.26 ± 7.42 μM and finally the IC_{90} without S9 of the compound **20** of 0.63 ± 0.04 μM was increased to 9.70 ± 0.87 μM. The potency observed for the compounds **1**, **10**, **13** and **14** that had a CF_3 moiety was not altered by addition of the S9 fraction.

Further study of the genotoxic properties was performed for the compounds **10**, **13** and **14** using a Comet assay [26]. With this assay, a fragmentation of the genomic DNA can be detected. Briefly, J774 A.1 cells were exposed to serial dilutions of the compounds and immobilized onto agarose. Immobilized cells were lysed and the remaining nuclei were submitted to electrophoresis. Through the pore exclusion of the agarose, fragmented DNA migrated further with the applied current. After staining with a gel red it can be observed that the genomic DNA of an undamaged nucleus maintains its spherical organization (HEAD) whereas fragmented DNA migrates further across the gel (TAIL). The ratio DNA in the TAIL/DNA in the HEAD is a measure of DNA fragmentation due to the genotoxicity of the compounds for the J774 A.1 murine macrophage like monocytes.

At low concentrations of 0.13 μM of the compound **10** there was a significant increase of an amount of DNA in the TAIL ($p < 0.0001$ Mann–Whitney test). The amount of DNA fragmentation was lower at 0.25 μM but still a significant increase ($p < 0.05$ Mann–Whitney test). The lower degree of DNA fragmentation at this concentration could be explained by cytotoxic effects caused by the compound. At 1.25 μM the concentration of the compound **10** exceeded its NI_{50} concentration and the results could not be interpreted. The results indicated fragmentation of the genomic DNA of the macrophages caused by the compound **10**. DNA fragmentation could not be detected by the COMET assay for 0.13, 0.25, 1.25, 2.50 and 5.00 μM of the compound **13**, but because of the exceeded NI_{50} values obtained with the NRU assay, the observations made at 12.50 μM were regarded inconclusive and omitted from Fig. 4. All concentrations 0.13, 0.25, 1.25, 2.50, 5.00, 12.50 and 25.00 μM of the compound **14** were studied in the COMET assay as well and no increase of DNA in the TAIL fraction could be observed. For the reason of genotoxicity and toxicity, the compounds **10** and **13** were omitted from the further study.

Macrophages are the major host cell for *M. tuberculosis* infection [27]. For most of its infectious cycle, *M. tuberculosis* resides within the early endosome of the macrophages where it replicates. Therefore it was important to investigate if the selected 1,3-diaryltriazene **14** is able to reach its target through the membrane structure of the macrophages. In the macrophage infection assay set up, cells were first infected with *M. tuberculosis* H37Rv^{lux}. After 24 h of infection, the infected J774 murine macrophages were treated with the compound **14** for 3 days. The treatment was followed by washing and the subsequent lysis of the J774 monolayer after a cell viability control by tryptophan blue staining. The luminescence emitted by the cell lysate was compared with infected macrophages which received no treatment. If the bacterial load inside the cells was diminished it was concluded that the compound was able to reach its target and kill it. As shown in Fig. 5, the compound **14** could indeed reduce the bacterial load inside the macrophages and after three days of exposure at 15.55 μM, the *M. tuberculosis* load inside the macrophage monolayer was reduced by 71.67%. At 7.79 μM the reduction still remained 62.02%. At 3.88 and 1.94 μM the reduction dropped to respectively 43.81% and 6.32% as compared to the bacterial load measured in the lysate from untreated *M. tuberculosis* infected macrophages.

To extend the study, antimicrobial activity against a multidrug resistant *M. tuberculosis* isolate was determined with the fluorometric BACTEC MGIT 960™ Mycobacteria Growth Indicator (Fig. 6) [28]. This standardized automated fluorometric assay relies an oxygen-quenched fluorochrome, tris(4,7-diphenyl-1,10-phenanthroline)ruthenium(II) chloride pentahydrate, embedded in silicone at the bottom of the tube. During a mycobacterial growth within the tube, free oxygen is utilized and is replaced with CO_2. With depletion of free oxygen, the fluorochrome is no longer inhibited, resulting in fluorescence within the MGIT tube when visualized under UV light. The intensity of a fluorescence is directly proportional to the extent of the oxygen depletion and the growth of the mycobacterial strain. Drug susceptibility can be measured in 4–6 days.

The growth inhibition induced by a compound was calculated by comparing the growth index of the *M. tuberculosis* culture exposed to different compound concentrations with the growth index of an untreated control culture 100 times diluted upon inoculation (C/100). As a resistant *M. tuberculosis* strain, a LAM-1 clinical isolate was selected. This MDR *M. tuberculosis* strain shows resistance against isoniazid, rifampicin, rifabutine and prothionamide. The susceptibility to the compound **14** was tested at a concentration range of 25.00 μM–1.25 μM. A growth index similar to the untreated control diluted 100 times upon inoculation, was found for a concentration between 12.5 μM and 6.25 μM, confirming the susceptibility of this MDR strain for the compound. INH did not inhibit the growth at the critical concentration of 0.73 μM, confirming the resistance of the strain towards this first line antibiotic.

3. Conclusions

A library of substituted 1,3-diaryltriazenes was synthesized in a convenient way followed by a biological evaluation for their

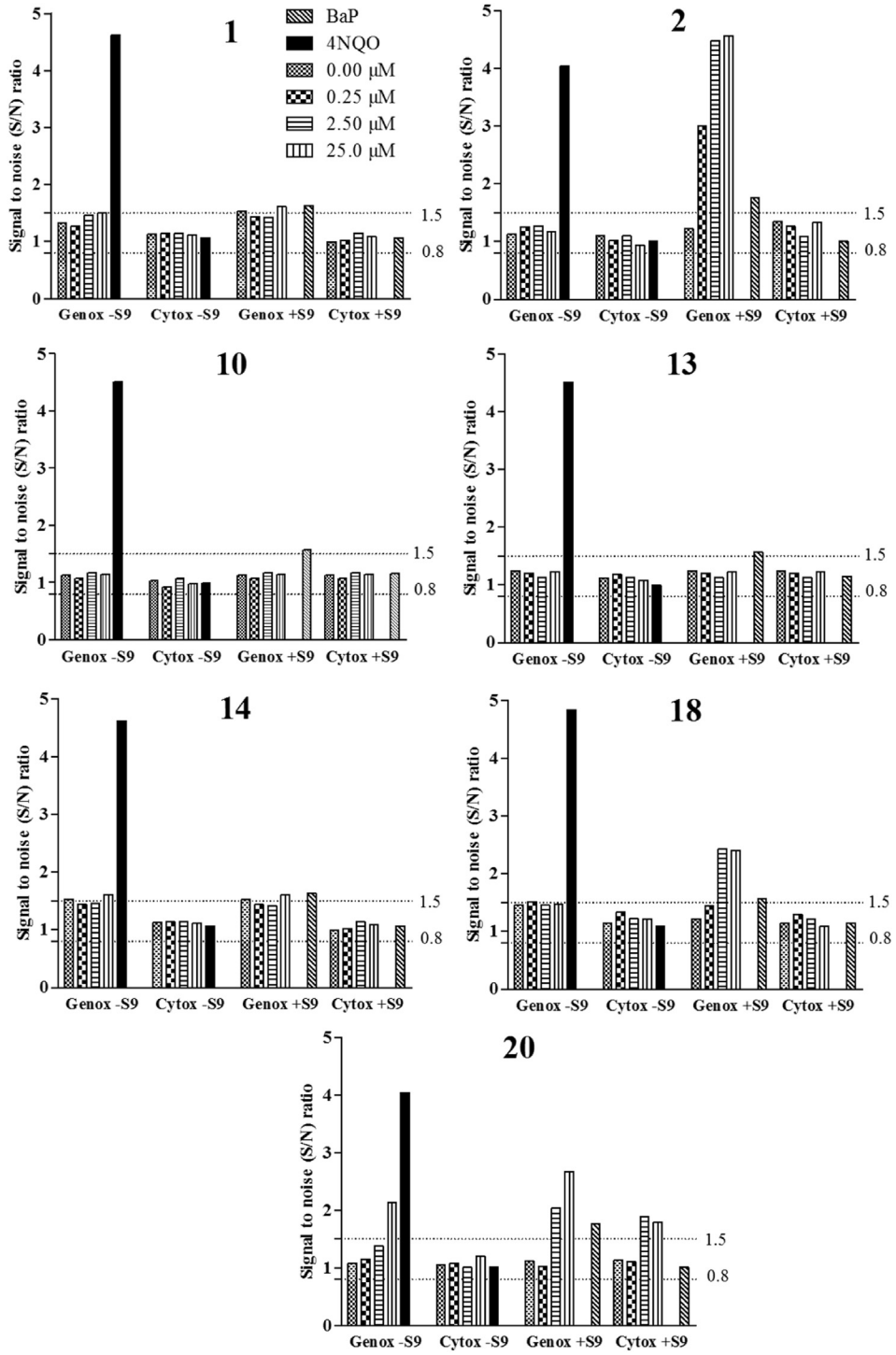

Fig. 2. The VITOTOX™ assay for the detection of early signs of genotoxicity caused by the compounds. Maximum recorded S/N in a time span of 4 h by the Genox (recN2-4) and Cytox (pr1) reporter strains. 4NQO; 4-nitroquinolone-1-oxide genotoxic positive control in samples without S9 liver fraction. Bap; benzo[*a*]pyrene, the positive control, only turns genotoxic after S9 metabolization.

potential as anti-tubercular agents. Several compounds were detected as 'hits' with an IC_{50} below 1 μM against *M. tuberculosis.* From the structure activity relation it could be deduced that compounds carrying a NO_2 group at the *para* R^4 position or a CF_3 functionality at the *meta* R^3 position were more active than analogues with alternative electron-withdrawing groups at those positions. Changing the position of these groups resulted in abrogation of the potency as well. The compounds selected for further testing showed a certain level of toxicity for J774 A.1 macrophages at low concentrations (30 μM) but due to the high potency of some, an acceptable selectivity index above 7 could be calculated for the compounds **1**, **2**, **10**, **13**, **14**, **18** and **20**. For these 1,3-diaryltriazenes the activity against *M. bovis*, *M. ulcerans* and two *M. avium* subspecies was confirmed, broadening their applicability. Genotoxicity was studied and detected for the compounds **2**, **18** and **20** after the addition of the S9 liver extract, but not in the absence of

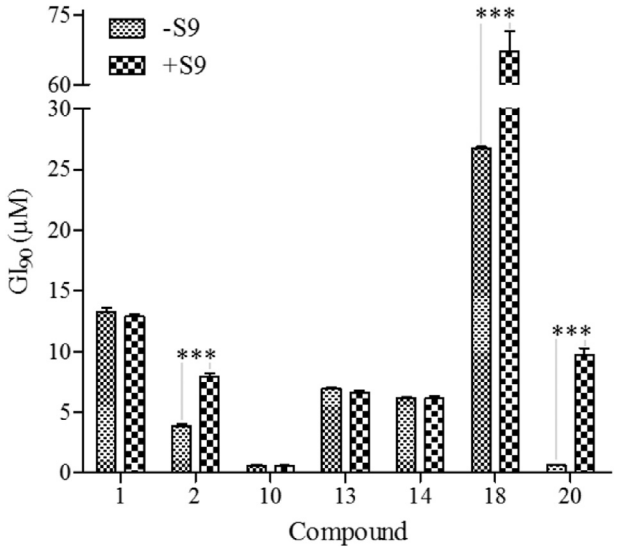

Fig. 3. The 90% *in vitro* growth inhibitory concentration of the derivatives against *M. tuberculosis* in the presence and in the absence of the S9. IC_{90}, the concentration at which 90% of the *M. tuberculosis* growth is inhibited, was measured in the presence and absence of the S9 liver extract. Results are shown as an average of the triplicate with SD bars. Significance was studied with Mann–Whitney test $p < 0.0001$.

S9. It indicated that a liver metabolism could be responsible for converting the compounds into genotoxic metabolites. This could not be observed for **1**, **10**, **13** and **14**. After analysis of the structural differences, it was found that the latter four compounds all carried a CF_3 functional group, preventing the metabolic destruction by the S9 extract. Next the MIC concentration against *M. tuberculosis* of the triazenes **1**, **2**, **10**, **13**, **14**, **18** and **20** was studied in the presence or in the absence of S9. It was observed that the potency of the derivatives **2**, **18** and **20** was significantly reduced and the molecules most probably metabolized in a non-potent metabolite whereas this was not the case for **1**, **10**, **13** and **14** where no reduction in efficacy was observed. This reinforced the importance of a CF_3 moiety as a functional group on these 1,3-diaryltriazene molecules. Further investigation of the possible genotoxic effects for the three most promising compounds showed that the compound **10** did indeed cause the DNA breakage and that for the triazene **13** the results were inconclusive due to cytotoxicity. In the case of **14**, the DNA breakage could not be observed at the concentrations tested. The compound **14** ($IC_{50} = 3.26$ μM, $NI_{50} = 24.22$ μM, $SI = 7.44$) was ultimately selected as the best representative of the library. In further studies it was found that this compound was able to inhibit

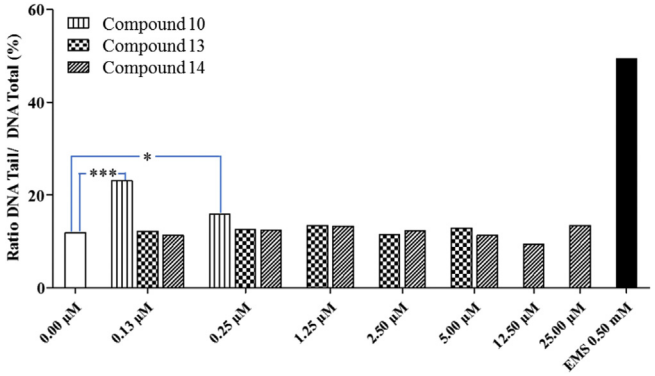

Fig. 4. Detection of DNA fragmentation by Comet assay. Genomic DNA fragmentation after 24 h exposure to the different concentrations of the compounds **10**, **13** and **14**. The Mann–Whitney *U* test was used to confirm the significance.

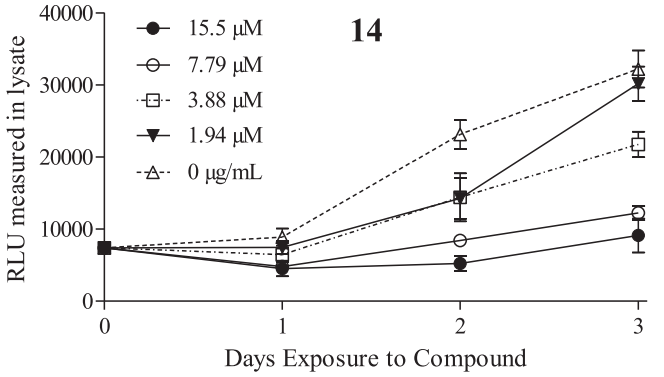

Fig. 5. Inhibition of an intracellular replication of *M. tuberculosis* inside macrophages by the compound **14**. Growth inhibition of *M. tuberculosis* H37Rv inside J774 A.1 macrophages. Results are presented as mean ± SD RLU of triplicate cultures. A treatment of the infected cells started 24 h post infection and lasted for 3 days.

the growth of a multi-drug resistant *M. tuberculosis* LAM-1 strain as well as the intracellular replication of *M. tuberculosis*, resulting in a growth reduction of 71.67% at 15.55 μM. As the anti-tubercular potency was accompanied with an acute cytotoxicity, combined with the DNA binding properties of the anti-trypanosomal drugs diminazene, the development of 1,3-dirayltriazenes should be done with caution. Given the fact that TB chemotherapy requires intensive treatment for several months, it is unlikely that these compounds could find their application as a first line drugs for the treatment of the drug susceptible strains. However with the increase in incidence of multi-, extensively- and total-drug resistant TB, when other treatment options are exhausted, this compound class might prove of use.

4. Experimental protocols

4.1. Chemistry

Starting materials for the synthesis of the examined compounds were used as obtained from the commercial sources (Aldrich, Fluka,

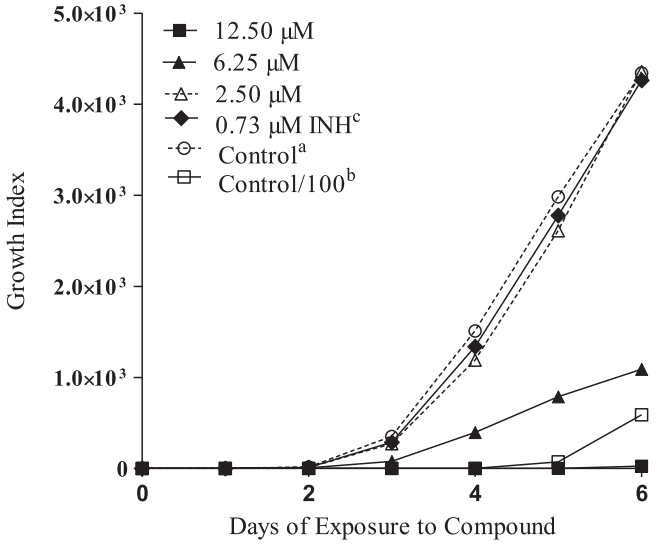

Fig. 6. Susceptibility of an MDR *M. tuberculosis* LAM-1 strain to the triazene **14**. Growth of MDR *M. tuberculosis* was monitored in BACTEC MGIT 960™. [a,b]Growth was compared to an untreated bacterial suspension and an untreated bacterial suspension diluted 100 times (C/100) to study the minimal inhibitory concentration MIC. [c] Resistance was confirmed with isoniazid (INH).

Alfa Aesar, Maybridge Chemical Company Ltd). Melting points were determined on a Kofler micro hot stage and are uncorrected. NMR spectra were recorded at 29 °C with a Bruker Avance DPX 300 spectrometer (^{1}H NMR spectra at 300 MHz; ^{13}C NMR spectra at 75.5 MHz) and with a Bruker Avance III 500 spectrometer (^{1}H NMR spectra at 500 MHz; ^{13}C NMR spectra at 125.8 MHz). Proton spectra are referenced to TMS as an internal standard; the carbon shifts are given against the central line of the solvent signal (DMSO-d_6 at $\delta = 39.5$ ppm; $CDCl_3$ at $\delta = 77.1$ ppm). In the ^{13}C NMR spectra of compounds **1**, **3**–**9**, **12** and **13** the resonances of were broadened to the baseline and are thus not reported. IR spectra were obtained with a Perkin–Elmer Spectrum 100, equipped with a Specac Golden Gate Diamond ATR as a solid sample support. MS spectra were recorded with an Agilent 6224 Accurate Mass TOF LC/MS spectrometer. Elemental analyses (C, H, N) were performed with Perkin Elmer 2400 Series II CHNS/O Analyzer. TLC was carried out on Fluka silica-gel TLC-cards.

All tested compounds possessed a purity of ≥95% as verified by NMR spectroscopy and elemental microanalysis. The figures, obtained from C, H, N analyses, were in all cases within ±0.35% of the calculated values.

4.1.1. General procedures for the synthesis of 1,3-diaryltriazenes

Method A: A solution of sodium nitrite (34.5 mg, 0.5 mmol) in water (3 mL) was added dropwise to the suspension of the appropriate aniline (1 mmol) in 5% water solution of HCl (2.5 mL) at 0 °C. The reaction mixture was stirred at room temperature for 18–23 h. Then, the solid material was filtered off and washed with water at 0 °C yielding the corresponding triazene.

Method B: A solution of isoamyl nitrite (117 mg, 1 mmol) in dichloromethane (4 mL; toluene, 2.5 mL in the case of 9) was added dropwise to the solution of the appropriate aniline (1 mmol) in dichloromethane (4 mL; petroleum ether, 2.5 mL in the case of 9) at 0 °C. The reaction mixture was stirred for 0.5–22 h at room temperature and evaporated to dryness under reduced pressure. Triazenes **8** and **9** were isolated by column chromatography. The crude products were always crystallized from the appropriate solvent.

Method C: A selected 3-arylpropenoic acid chloride (1.1 mmol) was slowly added to the mixture of the appropriate 1,3-diaryltriazene (1 mmol) and ethylamine (0.282 mL, 2 mmol) in acetone (5 mL). The reaction mixture was stirred at room temperature for 5–40 min. The product was isolated as follows: (a) Triethylamine hydrochloride was filtered off, the solution was evaporated to dryness and treated with a solvent (1 mL of methanol was used in the case of 21 and 25; 2 mL of methanol and 0.5 mL of acetone for the triazene 26) to obtain the desired product. (b) A solid material was separated by filtration, then suspended in water (2 mL) to remove triethylamine hydrochloride and the final product was filtered off (an isolation of **22** and **23**).

*4.1.1.1. 1,3-Bis[(2-fluoro-3-trifluoromethyl)phenyl]triazene (**1**).* Method A; reaction time: 20 h; yield: 75%; mp 111–113 °C (MeOH/H_2O); IR: 2988, 1633, 1596, 1535, 1489, 1470, 1418, 1325, 1313 cm^{-1}; ^{1}H NMR ($CDCl_3$): δ 7.22–7.33 (2H, m), 7.40–7.49 (2H, m), 7.83–7.93 (2H, m), 10.02 (1H, s); HRMS for $C_{14}H_8F_8N_3^+$ ($[M + H]^+$): calcd 370.0585, found 370.0586. Anal. for $C_{14}H_7F_8N_3$: calcd C, 45.54; H, 1.91; N, 11.38; found C, 45.33; H, 1.95; N, 11.32.

*4.1.1.2. 1,3-Bis[(2-fluoro-5-trifluoromethyl)phenyl]triazene (**3**).* Method A; reaction time: 20 h; yield: 98%; mp 125.1–126.3 °C (MeOH/H_2O); IR: 3313, 1622, 1611, 1530, 1513, 1489, 1478, 1448, 1413, 1335 cm^{-1}; ^{1}H NMR ($CDCl_3$): δ 7.23–7.34 (2H, m), 7.39–7.54 (2H, m), 7.91–8.00 (2H, m), 10.04 (1H, s); HRMS for $C_{14}H_6F_8N_3^-$ ($[M-H]^-$): calcd 368.0439; found 368.0438. Anal. for $C_{14}H_7F_8N_3$: calcd C, 45.54; H, 1.91; N, 11.38; found C, 45.29; H, 1.93; N, 11.31.

*4.1.1.3. 2,2′-(Triazene-1,3-diyl)-bis(6-fluorobenzonitrile) (**4**).* Method A; reaction time: 20 h; yield: 92%; mp 182.5–184.5 °C (MeOH/H_2O); IR: 3181, 2230, 1616, 1585, 1520, 1475, 1458, 1418 cm^{-1}; ^{1}H NMR ($CDCl_3$): δ 6.99–7.15 (2H, m), 7.54–7.68 (4H, m), 10.22 (s, 1H); HRMS for $C_{14}H_8F_2N_5^+$ ($[M + H]^+$): calcd 284.0742, found 284.0739. Anal. for $C_{14}H_7F_2N_5 \times 1/8H_2O$: calcd C, 58.90; H, 2.56; N, 24.53; found C, 58.84; H, 2.42; N, 24.23.

*4.1.1.4. 1,3-Bis(4-fluoro-2-(trifluoromethyl)phenyl)triazene (**5**).* Method A; reaction time: 19 h; yield: 84%; mp 155.3–157.5 °C (MeOH/H_2O); IR: 3358, 1612, 1592, 1522, 1483, 1449, 1433, 1420, 1320 cm^{-1}; ^{1}H NMR ($CDCl_3$): δ 7.22–7.32 (2H, m), 7.33–7.48 (2H, m), 7.62–7.89 (2H, m), 9.94 (1H, s); HRMS for $C_{14}H_8F_8N_3^+$ ($[M + H]^+$): calcd 370.0585, found 370.0581. Anal. for $C_{14}H_7F_8N_3$: calcd C, 45.54; H, 1.91; N, 11.38; found C, 45.54; H, 1.88; N, 11.40.

*4.1.1.5. 2,2′-(Triazene-1,3-diyl)-bis(5-fluorobenzonitrile) (**6**).* Method B; reaction time: 0.5 h; yield: 40%; mp 158–160 °C (MeOH/H_2O); IR: 3221, 2229, 1603, 1592, 1584, 1523, 1495, 1479, 1439, 1409 cm^{-1}; ^{1}H NMR (DMSO-d_6): δ 7.37–8.06 (6H, m), 13.44 (1H, s); HRMS for $C_{14}H_8F_2N_5^+$ ($[M + H]^+$): calcd 284.0742, found 284.0737. Anal. for $C_{14}H_7F_2N_5 \times 1/6H_2O$: calcd C, 58.74; H, 2.58; N, 24.47; found C, 58.76; H, 2.49; N, 24.23.

*4.1.1.6. 3,3′-(Triazene-1,3-diyl)-bis(6-fluorobenzonitrile) (**7**).* Method B; reaction time: 1.5 h; yield: 58%; mp 205–207 °C (petroleum ether/EtOAc); IR: 3285, 2235, 1613, 1600, 1582, 1522, 1487, 1454, 1405 cm^{-1}; ^{1}H NMR (DMSO-d_6): δ 7.46–8.30 (6H, m), 12.93 (1H, s); HRMS for $C_{14}H_6F_2N_5^-$ ($[M-H]^-$): calcd 282.0597, found 282.0591. Anal. for $C_{14}H_7F_2N_5 \times 1/8$EtOAc: calcd C, 59.19; H, 2.74; N, 23.80; found C, 59.26%; H, 2.73%; N, 23.83%.

*4.1.1.7. 1,3-Bis(4-fluoro-3-(trifluoromethyl)phenyl)triazene (**8**).* Method B; reaction time: 0.5 h; yield: 56%; mp 105.4–107 °C (petroleum ether); IR: 3339, 2987, 1618, 1513, 1493, 1464, 1421, 1321, 1304 cm^{-1}; ^{1}H NMR (DMSO-d_6): δ 7.43–8.09 (6H, m), 12.87 (1H, s); HRMS for $C_{14}H_8F_8N_3^+$ ($[M + H]^+$): calcd 370.0585, found 370.0582. Anal. for $C_{14}H_7F_8N_3$: calcd C, 45.54; H, 1.91; N, 11.38; found C, 45.70; H, 1.95; N, 11.31.

*4.1.1.8. N-(4-fluoro-3-nitrophenyl)-4-(3-(4-fluoro-3-nitrophenyl)triazene-1-yl)-2-nitroaniline (**9**).* Method B; reaction time: 22 h; yield: 37%; mp 193–195 °C (petroleum ether/EtOAc); IR: 3255, 2987, 1615, 1590, 1521, 1496, 1443, 1401, 1343, 1316 cm^{-1}; ^{1}H NMR (DMSO-d_6): δ 7.37–7.45 (1H, m), 7.57–7.67 (2H, m), 7.70–7.90 (3H, m), 8.00–8.21 (3H, m), 9.45 (1H, s), 12.86 (1H, s); HRMS for $C_{18}H_{12}F_2N_7O_6^+$ ($[M + H]^+$): calcd 460.0812, found 460.0812. Anal. for $C_{18}H_{11}F_2N_7O_6 \times 0.25C_2H_60$: calcd C, 47.19; H, 2.68; N, 20.82; found C, 47.31; H, 2.41; N, 20.59.

*4.1.1.9. 4,4′-(Triazene-1,3-diyl)-bis[2-(trifluoromethyl)benzonitrile] (**12**).* Method A; reaction time: 18 h; yield: 91%; mp 215–217 °C (MeOH/H_2O); IR: 2227, 1610, 1592, 1518, 1490, 1455, 1407, 1362, 1330, 1314 cm^{-1}; ^{1}H NMR ($CDCl_3$): δ 7.67–7.94 (6H, m), 10.14 (1H, s); HRMS for $C_{16}H_8F_6N_5^+$ ($[M + H]^+$): calcd 384.0678, found 384.0672. Anal. for $C_{16}H_7F_6N_5 \times 1/4H_2O$: calcd C, 49.56; H, 1.95; N, 18.06; found C, 49.76; H, 1.80; N, 17.67.

*4.1.1.10. 1,3-Bis[(4-nitro-3-(trifluoromethyl)phenyl)]triazene (**13**).* Method A; reaction time: 23 h; yield: 87%; mp 207–208 °C (MeOH/H_2O); IR: 3218, 1610, 1595, 1532, 1514, 1482, 1455, 1411, 1393, 1334, 1320 cm^{-1}; ^{1}H NMR (DMSO-d_6): δ 7.94–8.08 (4H, m), 8.23–8.31 (2H, m), 13.68 (1H, s); HRMS for $C_{14}H_8F_6N_5O_4^+$ ($[M + H]^+$): calcd 424.0475, found 424.0467. Anal. for $C_{14}H_7F_6N_5O_4 \times 1/3H_2O$: calcd C, 39.18; H, 1.80; N, 16.32; found C, 39.36; H, 1.59; N, 16.08.

*4.1.1.11. 3-[(2E)-3-(2,4-dimethoxyphenyl)prop-2-enoyl]-1,3-bis[(4-chloro-2-trifluoromethyl)-phenyl]-triazene (**21**).* Method C; reaction time: 5 min; yield: 80%; mp 154.5–156.5 °C (ethanol); IR:1682, 1603, 1566, 1359, 1310, 1260, 1214, 1162, 1134, 1049, 995 cm^{-1}; ^1H NMR ($CDCl_3$):δ 3.87 (3H, s), 3.91 (3H, s), 6.49 (1H, d, $J = 2.3$ Hz), 6.56 (1H, dd, $J = 2.3$, 8.6 Hz), 7.14 (1H, d, $J = 8.5$ Hz), 7.53–7.61 (2H, m), 7.62–7.72 (4H, m), 7.79 (1H, d, $J = 2.3$ Hz), 8.21 (1H, d, $J = 15.8$ Hz); ^{13}C NMR ($CDCl_3$): δ 55.50, 55.51, 98.5, 105.5, 113.5, 116.8, 119.3, 122.0, 122.4, 127.0, 127.6, 128.1, 130.4, 131.5, 132.6, 132.8, 132.9, 133.1, 134.9, 135.9, 142.4, 144.2, 160.5, 163.3, 167.8; MS (EI) *m/z* 591 (M^+, 11), 191 (100), 179 (22); Anal. for $C_{25}H_{17}Cl_2F_6N_3O_3$: calcd C, 50.69; H, 2.89; N, 7.09; found C, 50.86; H, 2.92; N, 6.88.

*4.1.1.12. 3-[(2E)-3-(2,4-dimethoxyphenyl)prop-2-enoyl]-1,3-bis[(4-chloro-3-trifluoromethyl)-phenyl]-triazene (**22**).* Method C; reaction time: 5 min; yield: 84%; mp 160–161 °C (ethanol); IR (KBr):1681, 1602, 1563, 1478, 1354, 1314, 1217, 1180, 1168, 1126, 1008 cm^{-1}; ^1H NMR ($CDCl_3$):δ 3.88 (3H, s), 3.92 (3H, s), 6.51 (1H, d, $J = 2.4$ Hz), 6.57 (1H, dd, $J = 2.4$, 8.5 Hz), 7.30 (1H, dd, $J = 2.4$, 8.5 Hz), 7.48–7.54 (2H, m), 7.58 (1H, d, $J = 8.6$ Hz), 7.66 (1H, d, $J = 8.5$ Hz), 7.67 (1H, dd, $J = 2.4$, 8.6 Hz), 7.74 (1H, d, $J = 15.8$ Hz), 7.92 (1H, d, $J = 2.4$ Hz), 8.14 (1H, d, $J = 15.8$ Hz); ^{13}C NMR ($CDCl_3$):δ 55.46, 55.52, 98.6, 105.5, 113.8, 116.8, 121.1, 122.4, 122.5, 126.5, 128.5, 129.4, 129.5, 132.36, 132.38, 132.39, 132.8, 133.1, 133.6, 134.5, 142.9, 146.9, 160.7, 163.3, 168.1; MS (EI) *m/z* 591 (M^+, 0.1), 191 (100), 148 (13); Anal. for $C_{25}H_{17}Cl_2F_6N_3O_3$: calcd C, 50.69; H, 2.89; N, 7.09; found C, 50.74; H, 2.96; N, 6.92.

*4.1.1.13. 3-[(2E)-3-(3,5-dimethoxyphenyl)prop-2-enoyl]-1,3-bis[(4-chloro-3-trifluoromethyl)-phenyl]-triazene (**23**).* Method C; reaction time: 5 min; yield: 73%; mp 158–160 °C (ethanol); IR: 1689, 1619, 1595, 1480, 1344, 1313, 1208, 1159, 1137, 1123 cm^{-1}; ^1H NMR ($CDCl_3$): δ 3.85 (6H, s), 6.56 (1H, dd, $J = 2.3$ Hz), 6.78 (2H, d, $J = 2.3$ Hz), 7.31 (1H, dd, $J = 2.4$, 8.4 Hz), 7.52 (1H, d, $J = 2.4$ Hz), 7.49–7.70 (4H, m), 7.91 (1H, d, $J = 2.4$ Hz), 7.91 (1H, d, $J = 15.7$ Hz); ^{13}C NMR ($CDCl_3$): δ 55.4, 103.1, 106.4, 116.2, 121.3, 122.3, 122.4, 126.4, 128.5, 129.4, 129.7, 132.5, 133.2, 133.4, 133.5, 134.0, 136.3, 146.5, 146.8, 161.2, 167.0; MS (FAB) *m/z* 592 ($[M+1]^+$, 1.0) 207 (100), 191 (72); Anal. for $C_{25}H_{17}Cl_2F_6N_3O_3$: calcd C, 50.69; H, 2.89; N, 7.09; found C, 50.77; H, 2.94; N, 7.01.

*4.1.1.14. 3-[(2E)-3-(4-acetoxy-3-methoxyphenyl)prop-2-enoyl]-1,3-bis[2-chloro-4-nitrophenyl]-triazene (**25**).* Method C; reaction time: 5 min; yield: 88%; mp 170–173 °C (methanol); IR: 1767, 1622, 1527, 1350, 1257, 1194, 1132, 1045, 1000 cm^{-1}; ^1H NMR ($CDCl_3$): δ 2.34 (3H, s), 3.89 (3H, s), 7.12 (1H, d, $J = 8.3$ Hz), 7.19 (1H, d, $J = 1.9$ Hz), 7.30 (1H, dd, $J = 1.9$, 8.1 Hz), 7.50 (1H, d, $J = 8.7$ Hz), 7.59 (1H, d, $J = 15.7$ Hz), 7.64 (1H, d, $J = 8.9$ Hz), 8.01 (1H, d, $J = 15.7$ Hz), 8.22 (1H, dd, $J = 2.4$, 8.9 Hz), 8.30 (1H, dd, $J = 2.4$, 8.7 Hz), 8.34 (1H, d, $J = 2.3$ Hz), 8.45 (1H, d, $J = 2.4$ Hz); ^{13}C NMR ($CDCl_3$): δ 20.6, 56.0, 112.6, 115.1, 120.2, 121.1, 122.72, 122.77, 123.5, 125.4, 126.1, 131.6, 132.3, 133.1, 134.4, 139.8, 142.2, 147.2, 147.8, 148.8, 149.4, 151.6, 166.0, 168.6; MS (EI) *m/z* 574 (M^+, 2.2), 154 (100), 136 (75), 71 (70), 55 (77); Anal. for $C_{24}H_{17}Cl_2N_5O_8$: calcd C, 50.19; H, 2.98; N, 12.19; found C, 50.44; H, 3.07; N, 11.86.

*4.1.1.15. 3-[(2E)-3-(4-acetoxy-3-methoxyphenyl)prop-2-enoyl]-1,3-bis[2-bromo-4-nitrophenyl]-triazene (**26**).* Method C; reaction time: 40 min; yield: 94%; mp 180–181 °C (diisopropyl ether/acetone); IR: 1769, 1699, 1623, 1527, 1467, 1347, 1256, 1193, 1150, 1121, 1038, 999 cm^{-1}; ^1H NMR (DMSO-d_6): δ 2.34 (3H, s), 3.90 (3H, s), 7.12 (1H, d, $J = 8.2$ Hz), 7.19 (1H, d, $J = 1.8$ Hz), 7.31 (1H, dd, $J = 1.8$, 8.2 Hz), 7.48 (1H, d, $J = 8.7$ Hz), 7.58 (1H, $J = 15.8$ Hz), 7.62 (1H, d, $J = 8.7$ Hz), 8.02 (1H, d, $J = 15.8$ Hz), 8.27 (1H, dd, $J = 2.4$, 8.7 Hz), 8.35 (1H, dd, $J = 2.4$, 8.7 Hz), 8.52 (1H, d, $J = 2.4$ Hz), 8.63 (1H, d, $J = 2.4$ Hz); ^{13}C NMR (DMSO-d_6): δ 20.4, 56.1, 113.5, 116.3, 120.8, 121.0, 121.4, 123.3, 123.4, 123.8, 124.1, 127.7, 128.5, 132.4, 133.0, 141.4, 141.9, 145.9, 147.7, 148.5, 149.8, 151.2, 165.9, 168.3; MS (FAB) *m/z* 662 ($[M+1]^+$, 0.2), 154 (100), 137 (70), 71 (46); Anal. for $C_{24}H_{17}Br_2N_5O_8$: calcd C, 43.46; H, 2.58; N, 10.56; found C, 43.65; H, 2.75; N, 10.30.

4.2. Biology

4.2.1. Materials

7H9 Growth medium was purchased as a powder from BD Science (Franklin Lakes, NJ, USA). DMEM, glutamax, non-essential amino acids, sodium pyruvate, gentamycin, 2-mercaptoethanol, PBS were from GIBCO Invitrogen (Carlsbad, CA, USA). OADC, mycobactin J, penicillin, fungizone and hygromycin were from Roche (Basel, CH) and Triton X-100, glycerol, Tween 80 and *n*-decanal were purchased from Sigma Aldrich (St. Louis, MO, USA).

Strains and growth conditions – *M. tuberculosis H37Rv* (American Type Culture Collection 27294) is known to be sensitive to the five first line anti-tuberculosis drugs (streptomycin, isoniazid, rifampin, ethambutol and pyrazinamide). The LAM-1 strain is a clinical isolate from a patient diagnosed with TB. This strain has been spoligotyped for identification and characterized for antibiotic resistance by the national TB reference lab of the Institute of Public Health of Belgium. With the resistance to isoniazid, rifampicin, rifabutin and prothionamid this strain was classified as a multi-drug resistant (MDR) strain. Four other strains used for screening were *M. bovis* strain AN5, *M. avium* ssp. *avium* ATCC 15769, *M. avium* ssp. *paratuberculosis* ATCC19698 and *M. ulcerans* 1615. All strains were cultivated in 7H9 medium supplemented with 10% oleic acid-albumin-dextrose-catalase (OADC) and 0.2% glycerol. For *M. bovis*, the glycerol was replaced with 0.05% Tween 80. The growth medium of *M. avium* ssp. *paratuberculosis* was further supplemented with mycobactin J (2 μg/mL) required for optimal *in vitro* growth. Both *M. avium* strains and the *M. bovis* strain were grown at 39 °C, *M. ulcerans* was grown at 32 °C and *M. tuberculosis* was grown at 37 °C.

4.2.2. Monitoring mycobacterial growth by luminometry

The minimal inhibitory concentration (MIC) against mycobacteria of all synthesized compounds was evaluated by testing serial dilutions. The *in vitro* assay was based on a method in which luminescent mycobacteria transformed with pSMT1 luciferase reporter plasmid is used. The tested compounds were solubilized in DMSO (Sigma–Aldrich) at stock concentrations of 10 mM. Serial dilutions of each compound were made in liquid 7H9 medium [Middlebrook 7H9 broth based (Difco)] + 10% FCS (Gibco). Volumes of 20 μL of the serial dilutions were added in triplicate to 96-well, flat-bottomed micro well plates. The bacterial suspension was made by thawing and dissolving a frozen Mycobacteria pellet in 7H9-10% FCS. The dissolved pellet was passed through a 5.0 μM filter (Millipore) to eliminate clumps and left for 1 h to recover at 37 °C, 5% CO_2. Next, the bacterial suspension was diluted in 7H9-10% FCS to obtain 50,000 Relative Light Units (RLU)/mL and a volume of 180 μL of bacteria was added to each well. A bacterial replication was analysed by luminometry after 6 days of incubation. The bacterial suspension from each well was collected, and transferred to a black 96-well plate to evade cross luminescence between wells. The luminescent signal was evoked by addition of the substrate for the bacterial luciferase, 1% n-decanal in ethanol to each well by the multi plus reader from Promega and the light emission in each well was measured.

4.2.3. Activity against multi-drug resistant M. tuberculosis

Antimicrobial activity of the compounds was tested using the LAM-1 strain using the BACTEC™ MGIT™ 960 TB detection system.

The compounds were dissolved in DMSO at stock concentrations of 1 mg/mL. Serial dilutions of each compound were made in 7H9 containing 10% OADC, at 83-fold the final concentrations. *M. tuberculosis* LAM-1 was pre-cultured in a 4 mL BACTEC vial to a growth index (GI) of 300. Then 100 μL of this pre-culture was inoculated into a new 4 mL BACTEC vial together with 100 μL of the serial dilutions of the compounds. As a positive control for the resistance, the MDR LAM-1 culture was inoculated with 0.1 μM isoniazid. The GI was measured each day. To determine the IC_{99}, the cultures, treated with the compounds were compared with an untreated culture diluted 100 times upon inoculation.

4.2.4. Inhibition of intracellular M. tuberculosis growth

The compounds were tested on the murine J774 A.1 macrophage cell line infected with *M. tuberculosis* H37Rv^{lux}. The J774 macrophages were grown at 37 °C, 5% CO_2 in complete DMEM medium until a semi confluent layer was formed. The macrophages were washed in fresh complete DMEM medium and seeded in a flat-bottomed 96-well micro well plate at a cell density of 40,000 cells per well. The cells were left to recover overnight and were washed three times in complete DMEM medium. *M. tuberculosis* H37Rv^{lux} was grown at 37 °C in 7H9 containing 10% FCS and 0.2% hygromycin to an OD_{580} of 0.6–1.0. The fully-grown bacterial suspension was measured and brought into complete DMEM-Pen/Fung [DMEM medium containing 0.1% penicillin and 0.8% fungizone but without gentamicin]. The synthesized compounds were dissolved in DMSO at stock concentrations of 10 mM. Serial dilutions of the peptides were made in DMEM-Pen/Fung at two times the concentration of each compound to be tested. A volume of 100 μL of the bacterial suspension in DMEM-Pen/Fung containing 4000 RLU of bacteria (multiplicity of infection of 0.1) and 100 μL of the serial compound dilutions were added to the macrophage cultures. To measure the effects of the compounds on intracellular growth of *M. tuberculosis*, the infected macrophages were washed three times on day 5 to remove all extracellular bacteria, incubated 1 h with 1% gentamicin to kill the residual extracellular bacteria, lysed with 200 μL 1% Triton X-100 (Sigma) and the wells washed four times with 200 μL PBS. The lysate was transferred in a 2.5 mL tube together with the 4 PBS washings. One hundred μL of 1% *n*-decanal in ethanol was added to the tube and the luminescence was measured. RLU values shown were obtained from six replicate cultures. Cell viability of the macrophage culture was observed by Trypan blue with a microscope.

4.2.5. Assessment of cytotoxicity

Inhibitory effects on the J774 A.1 murine macrophage cell line were determined for the derivatives by a neutral red uptake assay as described before. The J774 A.1 cells were grown in DMEM + 10% FCS until a semi confluent layer of cells was obtained. The cells were trypsinized, washed and 40,000 cells were seeded per well of a 96-well plate and left for recovery at 37 °C, 5% CO_2. The following days, the compounds were dissolved in DMSO to stock concentrations of 10 μM. A serial dilution of each compound was made in DMEM + 10% FCS. The J774 A.1 cells were washed and exposed to the derivatives by adding the serial dilutions of the compounds to the wells. The plates were left for incubation at 37 °C, 5% CO_2 for 24 h. After exposure, the cells were washed with 200 μL PBS and 200 μL neutral red working solution (Sigma) was added per well. Subsequently the plates were incubated for 3 h at 37 °C, 5% CO_2. The wells were washed with 200 μL PBS and 200 μL of an ethanol/acetic acid (50%) mixture. The plates were left on the shaker until the colour became homogeneous purple and the optical density was measured at 530 nm (NR max) and 620 nM (reference wavelength) with the Paradigm detection platform.

4.2.6. Vitotox assay

Observations on genotoxicity were done with Vitotox (Gentaur, Kampenhout, BE) and the included protocol was followed. In brief, TA104 RecN2-4 (genox) and TA104 (cytox) *Salmonella typhimurium* bacteria were cultivated at 36 °C for 16 h in poor 869 medium. The bacterial culture was diluted 250 times, incubated for 1 h at 36 °C and kept on ice. The bacterial culture was divided by 10 once more. S9 was added to the designated +S9 cultures to test the genotoxic effects of the metabolites of the compounds. The bacterial suspensions were then incubated, shaking at 36 °C, and the luminescent signal was measured for 4 h with a 5 min interval.

4.2.7. Comet assay

Possible DNA breakage effects of the derivatives on J774 A.1 cells were investigated by the alkaline comet assay. The J774 A.1 cells were grown in DMEM + 10% FCS until a semi confluent layer of cells was obtained. The cells were trypsinized, washed and seeded at 100,000 cells per well of a 24 well plate and left for recovery at 37 °C, 5% CO_2. The following day, the testing compounds were dissolved in DMSO as a stock concentration of 1 mM. Serial dilutions of each compound were made in DMEM + 10% FCS to obtain the final concentrations. The J774 A.1 cells were washed and exposed to the derivatives by adding 1 mL of the serial dilutions to each well. The plates were incubated at 37 °C, 5% CO_2 for 24 h. After incubation, the cells were trypsinized, washed with PBS, and 10 μL of cell suspension was dissolved in 300 μL low melting point agarose. The dissolved cell suspension was then placed onto a frosted microscope slide and left on ice for 5 min. The slide was subsequently placed in a jar containing lysing solution for 1 h. After lysis, the agarose cell suspension was subjected to electrophoresis for 20 min at 300 mA. The slides were washed with neutralization buffer for 5 min and dried in ice cold ethanol for 10 min. Staining of the DNA was done with gel red (Sigma–Aldrich). For the quantification of the DNA migration, a fluorescence microscope was used and the percentage DNA in the comet tail of the cells nuclei core was calculated in proportion to the total DNA present in the nuclei (comet head + tail) by appropriate imager software from Metasystems (Altlussheim, Germany).

Acknowledgements

This work was partially supported by the Research Foundation Flanders (FWO-Vlaanderen) (Grant G.0020.10N) and by funding from the European Community's Seventh Framework Program (FP7/2007-2013) under grant agreement FP7-223681. Slovenian Research Agency is gratefully acknowledged for the financial support (Project P1-0230). We thank Dr. Bogdan Kralj and Dr. Dušan Žigon (Mass Spectrometry Centre, Jožef Stefan Institute, Ljubljana, Slovenia) for recording some of the mass spectra. This work was also partly supported with the infrastructure of the EN-FIST Centre of Excellence, Dunajska 156, SI-1000 Ljubljana, Slovenia.

Appendix A. Supplementary data

Supplementary data related to this article can be found at http://dx.doi.org/10.1016/j.ejmech.2014.02.065.

References

[1] World Health Organization, Global Tuberculosis Report, 2012. http://www.who.int/tb/publications/global_report/en/.
[2] A.O. Ombaka, A.T. Muguna, J.M. Gichumbi, Antibacterial and antifungal activities of novel hydroxytriazenes, Journal of Environmental Chemistry and Ecotoxicology 4 (2012) 133–136.
[3] D.B. Kimball, M.M. Haley, Triazenes: a versatile tool in organic synthesis, Angewandte Chemie International Edition 41 (2002) 3338–3351.

[4] T.A. Connors, P.M. Goddard, K. Merai, W.C.J. Ross, D.E.V. Wilman, Tumor inhibitory triazenes - structural requirements for an active metabolite, Biochemical Pharmacology 25 (1976) 241–246.
[5] J.A. Hickman, Investigation of the mechanism of action of antitumour dimethyltriazenes, Biochimie 60 (1978) 997–1002.
[6] T. Fukushima, H. Takeshima, Anti-glioma therapy with temozolomide and status of the DNA-repair gene MGMT, Anticancer Research 29 (2009) 4845–4854.
[7] F. Marchesi, M. Turriziani, G. Tortorelli, G. Avvisati, F. Torino, L. De Vecchis, Triazene compounds: mechanism of action and related DNA repair systems, Pharmacological Research 56 (2007) 275–287.
[8] D.S. Pilch, M.A. Kirolos, X. Liu, G.E. Plum, K.J. Breslauer, Berenil [1,3-Bis(4′-amidinophenyl)triazene] binding to DNA duplexes and to a RNA duplex: evidence for both intercalative and minor groove binding properties, Biochemistry 34 (1995) 9962–9976.
[9] E.D. Clercq, O. Dann, Diaryl amidine derivatives as oncornaviral DNA polymerase inhibitors, Journal of Medicinal Chemistry 23 (1980) 787–795.
[10] T. Čimbora-Zovko, A. Brozovic, I. Piantanida, G. Fritz, A. Virag, B. Alič, V. Majce, M. Kočevar, S. Polanc, M. Osmak, Synthesis and biological evaluation of 4-nitro-substituted 1,3-diaryltriazenes as a novel class of potent antitumor agents, European Journal of Medicinal Chemistry 46 (2011) 2971–2983.
[11] B. Štefane, M. Kočevar, S. Polanc, Nitrosation with sodium hexanitrocobaltate(III), The Journal of Organic Chemistry 62 (1997) 7165–7169.
[12] J.A. Sweatlock, T.A. Gasiewicz, The interaction of 1,3-diaryltriazenes with the Ah receptor, Chemosphere 15 (1986) 1687–1690.
[13] D.T. Hill, K.G. Stanley, J.E. Karoglan Williams, B. Loev, P.J. Flower, J.P. McCafferty, E. Macko, C.E. Berkoff, C.B. Ladd, 1,3-Diaryltriazenes: a new class of anrectic agents, Journal of Medicinal Chemistry 26 (1983) 865–869.
[14] G. Vernin, C. Siv, J. Metzger, C. Párkányi, Synthesis of 1,3-diaryltriazenes and their derivatives by aprotic decomposition of arylamines, Synthesis (1977) 691–693.
[15] A. Virag, A. Meden, M. Kočevar, S. Polanc, Synthesis and characterization of new triazenide salts, The Journal of Organic Chemistry 71 (2006) 4014–4017.
[16] D. Cappoen, J. Jacobs, V.T. Nguyen, S. Claesens, G. Diels, R. Anthonissen, M. Fauville, L. Verschaeve, K. Huygen, N. De Kimpe, Straightforward palladium-mediated synthesis and biological evaluation of benzo[j]phenanthridine-7,12-diones as anti-tuberculosis agents, European Journal of Medicinal Chemistry 48 (2012) 57–68.
[17] D. Forge, D. Cappoen, D. Stanicki, T. Huang, L. Verschaeve, K. Huygen, J.J. Vanden Eynde, 1,4-Diarylpiperazines and analogs as anti-tubercular agents: synthesis and biological evaluation, European Journal of Medicinal Chemistry 49 (2012) 95–101.
[18] D. Cappoen, D. Forge, F. Vercammen, V. Mathys, M. Kiass, V. Roupie, R. Anthonissen, L. Verschaeve, J.J. Vanden Eynde, K. Huygen, Biological evaluation of bisbenzaldehydes against four *Mycobacterium* species, European Journal of Medicinal Chemistry 63 (2013) 731–738.
[19] P. Claes, D. Cappoen, B. Mbala, J. Jacobs, B. Mertens, V. Mathys, L. Verschaeve, K. Huygen, N. De Kimpe, Synthesis and antimycobacterial activity of analogues of the bioactive natural products sampangine and cleistopholine, European Journal of Medicinal Chemistry 67 (2013) 98–110.
[20] G. Repetto, A. del Peso, J.L. Zurita, Neutral red uptake assay for the estimation of cell viability/cytotoxicity, Nature Protocols 3 (2008) 1125–1131.
[21] J.J. Cortez-Escalante, A.M. Santos, G.C. Garnica, A.L. Sarmento, C.N. Castro, G.A.S. Romero, Mediastinitis and pericardial effusion in a patient with AIDS and disseminated *Mycobacterium avium* infection: a case report, Revista da Sociedade Brasileira de Medicina Tropical 45 (2012) 407–409.
[22] R.J. Chiodini, W.M. Chamberlin, J. Sarosiek, R.W. McCallum, Crohn's disease and the mycobacterioses: a quarter century later. Causation or simple association? Critical Reviews in Microbiology 38 (2012) 52–93.
[23] T. Einarsdottir, K. Huygen, Buruli ulcer, Human Vaccines 7 (2012) 1198–1203.
[24] G.S. Hotter, D.M. Collins, Mycobacterium bovis lipids: virulence and vaccines, Veterinary Microbiology 151 (2011) 91–98.
[25] L. Verschaeve, J. Van Gompel, L. Thilemans, L. Regniers, P. Vanparys, D. Van der Lelie, VITOTOX® bacterial genotoxicity and toxicity test for the rapid screening of chemicals, Environmental and Molecular Mutagenesis 33 (1999) 240–248.
[26] R.R. Tice, E. Agurell, D. Anderson, B. Burlinson, A. Hartmann, H. Kobayashi, Y. Miyamae, E. Rojas, J.C. Ryu, Y.F. Sasaki, Single cell gel/comet assay: guidelines for in vitro and in vivo genetic toxicology testing, Environmental and Molecular Mutagenesis 35 (2000) 206–211.
[27] M.J. Fenton, M.W. Vermeulen, Immunopathology of tuberculosis: roles of macrophages and monocytes, Infection and Immunity 64 (1996) 683–690.
[28] B.A. Hanna, A. Ebrahimzadeh, L.B. Elliot, M.A. Morgan, S.M. Novak, S. Rusch-Gerdes, M. Acio, D.F. Dunbar, T.M. Holmes, C.H. Rexen, C. Savthyakumar, A.M. Vannier, Multicenter evaluation of the BACTEC MGIT 960 system for recovery of mycobacteria, Journal of Clinical Microbiology 37 (1999) 748–752.